Determining Rock Varieties on The Basis of Fuzzy Clustering of Ultrasonic Measurement Results

Volodymyr Morkun[a], Gerhard Fischerauer[b], Natalia Morkun[a], Vitaliy Tron[a] and Alona Haponenko[a]

[a] *Kryvyi Rih National University, Vitalii Matusevich street,11, Kryvyi Rih, 50027, Ukraine*
[b] *Bayreuth University, Universitätsstraße 30, Bayreuth, 95447, Germany*

Abstract

Geophysical methods of investigating rocks are used to define the geological structure of mineral resources by borehole sections, identify and evaluate iron ore raw materials. Geophysical data can be also applied to designing, controlling and analyzing deposit mining and engineering states of mine workings.

The research is aimed at improving accuracy of ultrasonic logging to determine physical-mechanical and chemical-mineralogical characteristics of rocks based on the fuzzy clustering of the results of ultrasonic measurements: velocity of longitudinal and transverse wave propagation, the ultrasonic attenuation coefficient at fundamental frequency and higher harmonics and relationship of these parameters.

Keywords

Iron ore, identification, ultrasound, fuzzy, clustering

1. Introduction

In Ukraine, balance reserves of iron ore amount to over 30 billion tons, which is sufficient to supply mining and metallurgical enterprises for about 95-100 years ahead. Of ten large-scale iron ore mining enterprises of the country, seven are located in Kryvyi Rih region: the CJSC *Inhuletskyi GZK*, the PJSC *Pivdennyi GZK*, the Mining Department of the PJSC *ArcelorMittal Kryvyi Rih*, the PJSC *Tsentralnyi GZK*, the PJSC *Pivnichnyi GZK*, the PJSC *Kryvbasrudkom*, and the PJSC *Sukha Balka*. These enterprises of Kryvyi Rih iron ore basin provide more than 90% of Ukrainian metallurgical enterprises' needs in raw materials [1].

In general, iron ores are represented by three main types – rich martite, ferruginous quartzite and brown ironstone. Ferruginous quartzites, which are the main reserve for developing the raw material base of Kryvyi Rih basin, belong to the hard-rock geological and industrial type. Depending on the availability of certain layers, magnetite ferruginous quartzites are divided into a number of varieties characterized by a different technological value: magnetite quartzite containing almost no silicates and carbonates; silicate-magnetite quartzite with subordinate quantity of silicate layers; hematite-iron-mica-magnetite quartzite with subordinate quantity of hematite layers; magnetite-silicate quartzite with subordinate quantity of magnetite layers, poor quartzite on the verge of industrial significance; carbonate-magnetite quartzite; silicate-carbonate, or carbonate-silicate magnetite quartzite.

The efficiency of mining and processing enterprises depends on how accurately and timely they receive information on geological and mineralogical types of iron ore raw materials that are extracted or processed. To obtain information on geological and mineralogical types of iron ore raw materials, there are applied methods of geophysical research based on various measurements of rock properties

IntelITSIS'2021: 3rd International Workshop on Intelligent Information Technologies and Systems of Information Security, March 23–25, 2021, Khmelnytskyi, Ukraine
EMAIL: morkunv@gmail.com (V. Morkun); MRT@uni-bayreuth.de (G. Fischerauer); nmorkun@gmail.com (N. Morkun); vtron@knu.edu.ua (V.Tron); a.haponenko@protonmail.com (A. Haponenko)
ORCID: 0000-0003-1506-9759 (V. Morkun); 0000-0003-2000-4730 (G. Fischerauer); 0000-0002-1261-1170 (N. Morkun); 0000-0002-6149-5794 (V.Tron); 0000-0003-1128-5163 (A. Haponenko)

as well as related data obtained when performing various technological operations, such as drilling boreholes.

Xiaowei Pan [2], Victor Mwango Bowa [3] suggest an approach to static optimization of drilling processes in the context of ore mining and processing, yet little attention is paid to dynamic processes occurring directly in borehole drilling. Z.Q. Yue, C.F. Lee, K.T. Law, and L.G. Lam [4] indicate that the mechanical drilling rate is a sufficient dynamic indicator characterizing rock properties. The disadvantage of this approach is that in the complex geological structure of iron ore deposits, this indicator is insufficient and requires analysis of a large number of variables to confirm research results [5,6].

H. Schunnesson [6] suggests determining a rock type in the course of drilling by two indicators – a mechanical drilling (penetration) rate and torque. The disadvantage of this approach is that the required accuracy of rock type recognition can be achieved in a binary geological structure, because these parameters indicate homogeneity and strength of the rock quite accurately. With several mineralogical and technological varieties available, this approach is difficult to apply.

Natalie Beattie [7] applies the following parameters to monitoring the drilling process: horizontal and vertical vibrations, axial pressure, torque, drilling rate, rotation rate, etc. The disadvantage of this approach is that among the controlled parameters there are only those of a drilling rig and no directly or indirectly measured characteristics of the drilled rock. Jorge Martin [8] uses a similar approach to identify a ternary geological structure using three types of drilled rocks. However, as in the above work, rock varieties are mainly identified by a single indicator (strength) and drilling rig parameters without measuring characteristics of the rock itself.

Ultrasonic measurements are promising for rapid determination of geological and mineralogical types of iron ore raw materials.

Ultrasonic logging is based on elastic wave propagation in the studied medium to determine its physical-mechanical and chemical-mineralogical characteristics [11,10]. Acoustic waves in solids can be divided into volume, surface, waveguide and guided. Volume acoustic waves propagate throughout the solid. The shape of the wave front is one of their distinguishing features [11,12]. They can be flat, spherical, cylindrical, etc. Another feature is the direction of the shear vector of particles of the medium, on this basis there are distinguished volume-longitudinal and volume-transverse waves. Surface acoustic waves propagate near the free surface of a solid body or near the interface between two different media [13]. Their phase velocity is parallel to this surface and their intensity decreases rapidly with the depth of penetration into the volume of the solid. Waveguide acoustic waves can exist in rods and thin layers as in waveguides, and guided waves – in protrusions or grooves of different profiles on the surface of a solid body as in channels.

2. Proposed methodology

Let us consider the method of determining geological and mineralogical varieties of rocks based on assessment of changes in the velocity of longitudinal and transverse volume ultrasonic waves, a relationship of these values in the controlled medium, as well as a parameter characterizing the degree of nonlinearity of this process – the value of ultrasound attenuation on fundamental and higher harmonics.

In rocks, propagation velocities of elastic waves vary widely and depend on physical properties, structure, texture, condition and other internal and external factors. Propagation velocities of elastic waves in the unlimited elastic medium can be determined by formulas derived from wave equations [14]. The velocity of the longitudinal wave in the bulk is

$$C_L = \sqrt{\frac{E}{\rho} \cdot \frac{1-\sigma}{(1+\sigma)\cdot(1-2\sigma)}} \tag{1}$$

where ρ is the density of the medium, E is the Young modulus, and σ is the Poisson ratio.

The transverse-wave propagation velocity is

$$C_T = \sqrt{\frac{E}{\rho} \cdot \frac{1}{2\cdot(1+\sigma)}} = \sqrt{\frac{\mu}{\rho}} \tag{2}$$

where μ is the shear modulus.

The ratio of the velocity of longitudinal waves to that of the transverse ones is a function only of the Poisson ratio of the rock:

$$\frac{C_L}{C_T} = \sqrt{2 \cdot \frac{1-\sigma}{1-2\sigma}}. \quad (3)$$

Propagation velocities of elastic waves in rocks vary significantly depending on mineral composition, density, porosity, grain size, and other parameters. Their values increase from acidic intrusive rocks to basic and ultrabasic ones. In igneous rocks, a decrease in values of propagation velocities of elastic waves with increasing SiO_2 content is noticeable. In rocks of basic composition, the velocity of longitudinal waves in intrusive samples is on average 20% higher than in effusive ones. As acidity increases, this difference decreases. There is no such relationship for transverse-wave velocities [15]. The propagation velocities of longitudinal and transverse elastic waves for igneous and metamorphic rocks are linearly related to density. No such regularities are established for sedimentary rocks. The values of elastic wave velocities change due to variable structural and textural characteristics of rocks in different places of sampling for testing. Thus, the coefficient of velocity variation of longitudinal waves in rocks taken from one deposit amounts to up to 40% in clays and up to 25% in limestones and dolomites. The distribution of values of elastic wave velocities in most igneous and metamorphic rocks follows a Gaussian normal distribution [16,17].

Table 1 shows statistical characteristics of elastic properties of the most common rocks and ultrasound velocities in them.

Table 1

Statistical characteristics of elastic properties of the most common rocks and ultrasound velocities in them

Parameters	Min	Max	Mean	Median	Variance	Standard Deviation
C_L, m/s	4450.0000	6320.0000	5562.2222	5930.0000	556094.4444	745.7174
C_T, m/s	2780.0000	3370.0000	3123.3333	3140.0000	40175.0000	200.4370
ρ, g/cm³	2.5200	2.9600	2.7211	2.7000	0.0187	0.1366
E, hPa	47.7451	85,9804	66,9935	70,9804	159,3946	12,5008
μ, hPa	20.1961	32.7451	26.5359	27.0588	175.9804	4.1432
σ	0.1800	0.3200	0.2582	0.3050	0.0040	0.0636

As follows from Fig. 1 and Fig. 2, the velocities of longitudinal and transverse ultrasonic waves in rocks are determined by their elastic characteristics:

- the velocity of longitudinal waves increases with the Young modulus and the Poisson ratio;
- changes in the Poisson ratio from 0.1 to 0.4 increase the longitudinal wave velocity by about 45%.
- the velocity of transverse waves increases with the Young modulus, but decreases with the Poisson ratio.

The dependence on the material parameters is non-linear as shown by eqns. (1), (2), but it can be linearized in sufficiently narrow intervals. Such regression lines have been drawn in Figs. 1 and 2. Thus, the velocity of elastic wave propagation in rocks is determined by their elastic properties and density. This velocity is almost independent of the wavelength, which enables using waves with any frequency for research.

In contrast to the velocity of elastic wave propagation, the physical dispersion of which is almost absent in most rocks, the attenuation coefficient is determined by the frequency of elastic oscillations. In a wide range of frequencies from 1 Hz to 10 MHz, the attenuation coefficient *a* in different rocks varies from $1 \cdot 10^{-8}$ to $2 \cdot 10^{2}$ m^{-1}. The attenuation decrement in the same frequency range varies from $1 \cdot 10^{-2}$ to 1.0 on the average.

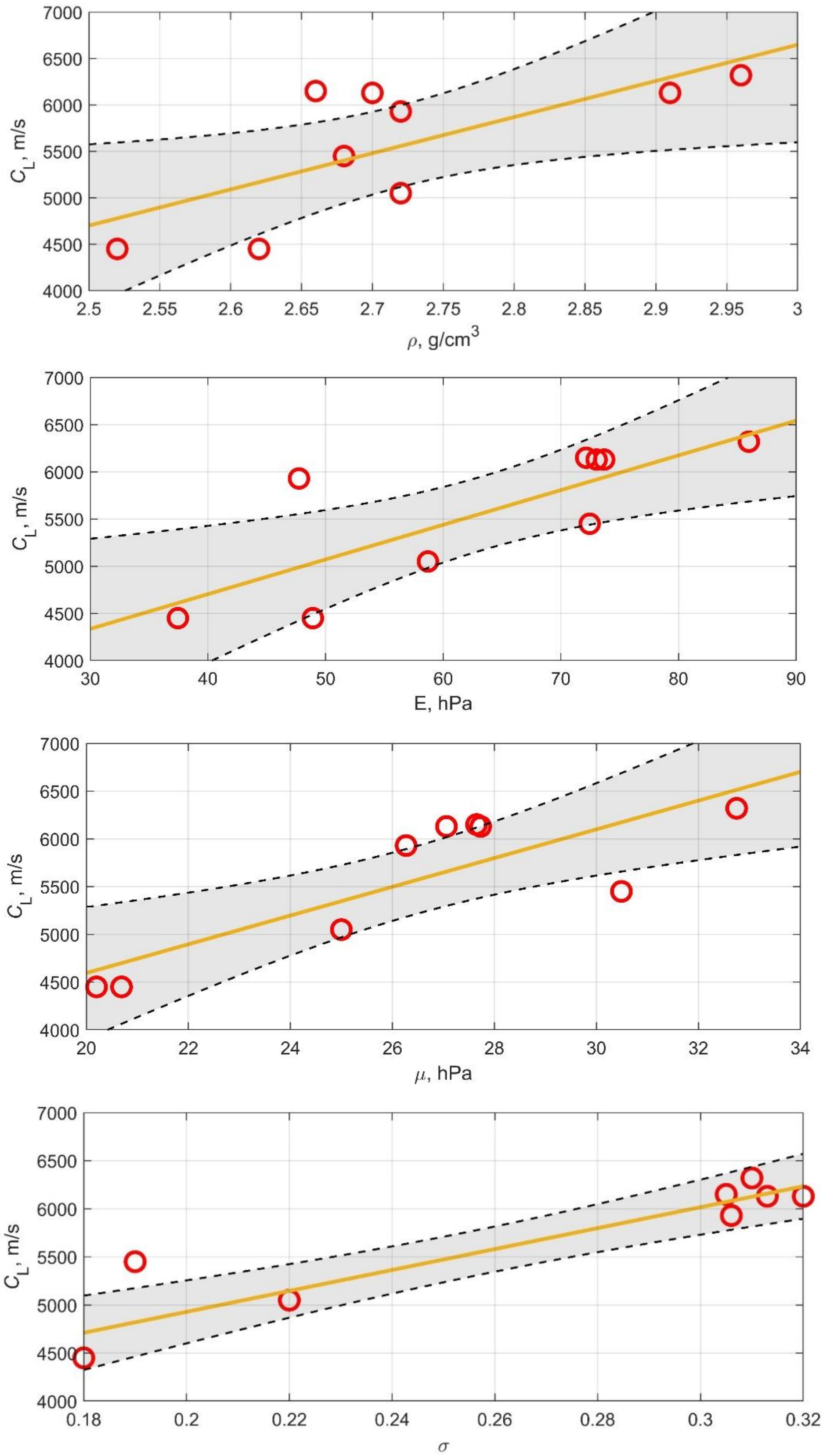

Figure 1: Dependence of the velocity of longitudinal ultrasonic waves, C_L, on rock characteristics. The shaded bands are the Working-Hotelling uncertainty intervals of the regression lines at the 95% confidence level.

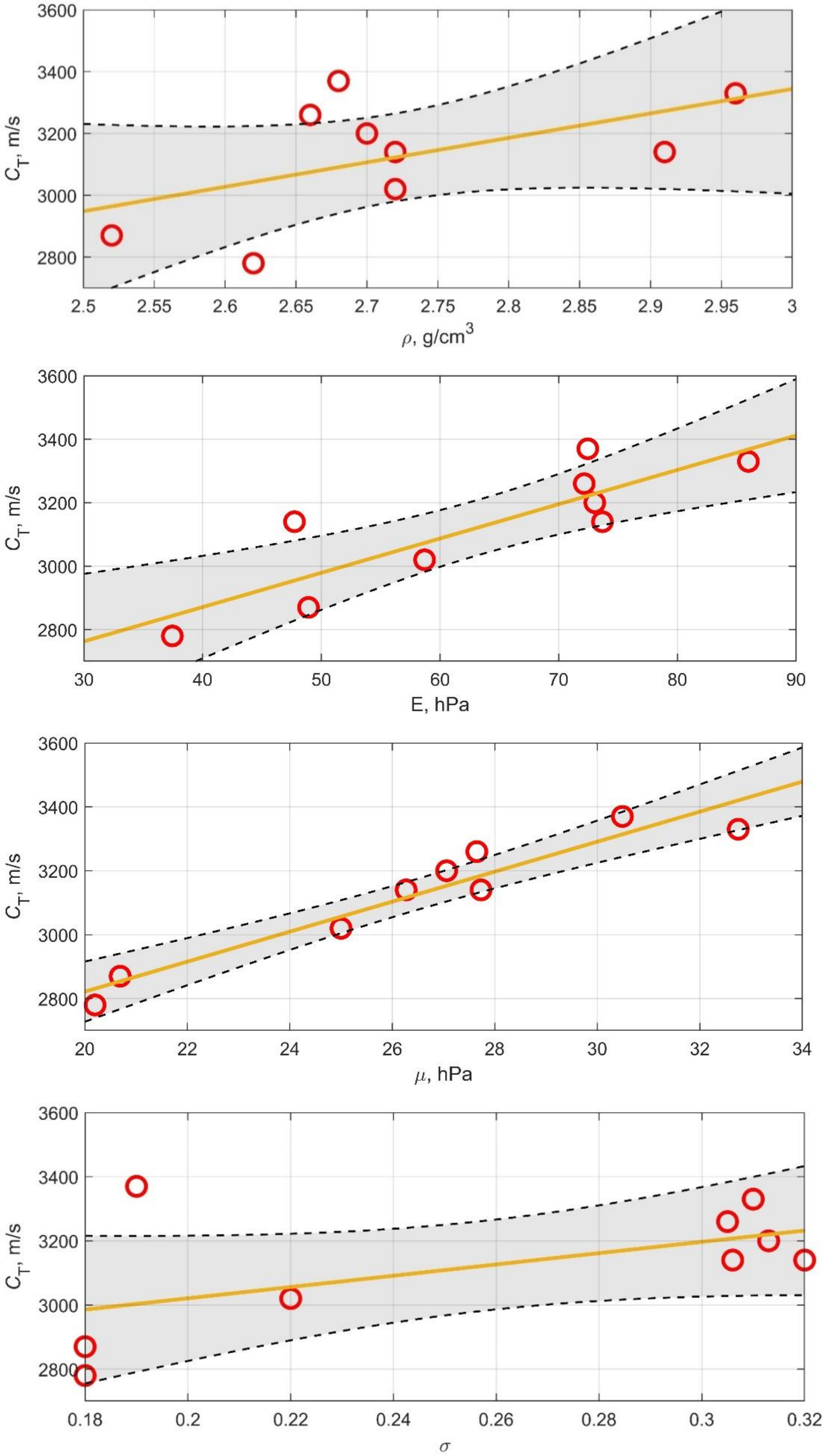

Figure 2: Dependence of the velocity of transverse ultrasonic waves, C_T, on rock characteristics. The shaded bands are the Working-Hotelling uncertainty intervals of the regression lines at the 95% confidence level.

The attenuation coefficient increases with frequency. However, a clear unambiguous functional dependence of attenuation on frequency for rocks is not established. For example, for granites in the frequency range from 10 kHz to 1000 kHz, the best approximation is observed when describing the frequency dependence by the quadratic function $\alpha=mf^2$, where m is the coefficient of proportionality. In gabbro-diabases, quartzites, granite-gneisses, sandstones, shales and other rocks, the frequency dependence in the range from 500 kHz to 5000 kHz obeys the law $\alpha=A_1f+A_2f^2$. This dependence is observed for both longitudinal and transverse waves [15,16].

Table 2 contains statistical characteristics of elastic properties of the most common rocks and the attenuation of ultrasonic waves in them. Table 3 summarizes the calculated correlation coefficients between basic parameters of ultrasonic waves propagating in rocks considering their attenuation.

Table 2
Statistical characteristics of elastic properties of the most common rocks, velocities of propagation, and attenuation of ultrasonic waves in them.

Parameters	Min	Max	Mean	Median	Variance	Standard Deviation
α, dB/m	4.0000	71.0000	35.6250	35.5000	563.1250	23.7303
C_L, m/s	4144.0000	5714.0000	4768.8750	4620.0000	401339.5536	633.5137
C_T, m/s	2343.0000	2857.0000	2652.6250	2731.0000	40868.5536	202.1597
ρ, g/cm³	2.6000	3.0550	2.75350	2.7050	25.6934	0.1603
E, hPa	34.4400	59.8700	47.7438	47.9350	97.2451	9.8613
σ	0.1500	0.3300	0.2588	0.2650	0.0036	0.0601

Table 3
Correlation coefficients between basic parameters of ultrasonic wave propagation in rocks considering their attenuation.

Parameters	α, dB/m	C_L/C_T	C_L, m/s	C_T, m/s	ρ, g/cm³	E, kg/mm²	σ
α, dB/m	1.0000	0.0200	0.1905	0.3328	0.5132	0.3582	-0.1356
C_L/C_T	0.0200	1.0000	0.8379	0.2815	0.6962	0.6273	0.9732
C_L, m/s	0.1905	0.8379	1.0000	0.7591	0.6393	0.9130	0.7743
C_T, m/s	0.3328	0.2815	0.7591	1.0000	0.3105	0.8623	0.2014
ρ, g/cm³	0.5132	0.6962	0.6393	0.3105	1.0000	0.6514	0.6670
E, hPa	0.3582	0.6273	0.9130	0.8623	0.6514	1.0000	0.5697
σ	-0.1356	0.9732	0.7743	0.2014	0.6670	0.5697	1.0000

In crystalline rocks, the attenuation coefficient of transverse waves is usually equal to that of longitudinal waves or about 1.5–2 times higher. In wet clays and water-saturated sands, there is a significant difference in attenuation coefficients of transverse and longitudinal waves (up to 5 or more) [15,16]. It should be noted that when velocities of elastic wave propagation in many hard monolithic rocks change by 40%–60%, their attenuation coefficients change by a factor of 2–4. Thus, this indicates that the attenuation coefficient of elastic waves is a more sensitive parameter for qualitative characteristics of rocks than the velocity of ultrasound. However, this factor causes a dependence of attenuation of ultrasonic oscillations that propagate in the studied medium on a variety of disturbing factors, such as changes or violations of its structure.

Ultrasonic methods of measuring characteristics of rocks with phase inhomogeneity such as cracks and pores face a number of difficulties due to the fact that in this case ultrasonic propagation becomes significantly nonlinear. In this case, the fundamental assumption that constitutive behaviour of a material under study is linear-elastic which is justified for linear measurements is not true. Most rocks are not linearly elastic even before formation of cracks. More importantly, nonlinear elasticity of rocks increases significantly with available cracks and pores [18].

Porosity as presence of pores, cracks (voids) in rocks is one of their most important structural features. Total (absolute, physical, complete) porosity is characterized by the ratio of the pore volume to that of the whole rock. The coefficient of total porosity k_t is a ratio of the volume of all pores V_p to the total volume of the rock sample V_r in fractions or percentages

$$k_t = \frac{V_p}{V_r} \cdot 100. \quad (4)$$

According to their origin, pores and cracks can be primary or secondary. The first are pores and cracks formed during sedimentation and formation of the rock massif. Secondary pores and cracks are formed during post-diagenetic changes.

From research results [19] it can be concluded that velocities of longitudinal and transverse ultrasonic waves have a significant dependence on porosity.

According to mechanics of elastic waves, ultrasound causes a slight deformation of tension and compression inside the rock, with friction occurring during compression strains. The contact area between crack surfaces and pore surfaces is a set of irregularities that are in close proximity to each other, which, for example, corresponds to the grain contact pattern characteristic of sedimentary rocks [20]. The energy dissipated at each irregularity can be written as follows [21]

$$W_f = \alpha\, \tau_f\, \sigma, \quad (5)$$

where τ_f is shear stress on the crack surface caused by ultrasound, σ is compression stress, a is the length of the contact between irregularities of the crack.

It follows from the above that available cracks and pores in the structure of the material cause strongly nonlinear dynamic phenomena accompanying propagation of elastic waves, and, consequently, changes in characteristics (propagation rate, attenuation) of this process.

Thus, there arises a need to study nonlinearity of the process of ultrasound propagation in rocks and take into account the influence of cracks and pores on the results of measuring characteristics of this process.

In the process of movement, the shape of the wave train changes: there is a decrease in the height of the envelope of the ultrasonic signal while increasing its width (spread of the wave train in space caused by dispersion properties of the medium).

Generation of higher harmonics is a traditional phenomenon, when the shape of the incident wave is distorted by a nonlinear elastic response of the medium to this wave. When sending a purely sinusoidal ultrasound signal with amplitude A_0 at frequency f_0, the detected signal passing through the defect will be distorted, and the detected wave will have the amplitude component A_1 at fundamental frequency f_0, the amplitude component A_2 at the second harmonic frequency $2f_0$, A_3 at the third harmonic frequency $3f_0$, etc.

In [21] the solution of the second-order nonlinear wave equation is approximated to obtain the following expression of the quadratic nonlinearity parameter:

$$\beta_n = \frac{8A_2}{A_1^2 k^2 x}, \quad (6)$$

where A_1 and A_2 are the frequency amplitudes of the first and second harmonics of the recorded signals, respectively; k is the wave number, x is the propagation distance.

Similarly, the third-order nonlinear coefficient of elasticity is expressed as

$$\gamma = \frac{48A_3}{A_1^3 k^3 x}, \quad (7)$$

where A_3 is the third harmonic amplitude.

As a rule, as the damage to the test material increases, the degree of nonlinear interaction also increases, and energy is transferred from the fundamental frequency to higher harmonics. Thus, damages and their quantitative characteristics can be assessed by measuring the nonlinearity of the ultrasonic wave propagating through the material.

The longitudinal ultrasonic wave propagates through the contact between two hard surfaces of medium particles. The availability of cracks and pores in the test samples causes modulation of the propagating ultrasonic train. The formation of the harmonic frequency that is twice the frequency of the main input signal is caused by an incorrect waveform in the time domain after a certain propagation distance covered. The ultrasonic wave is distorted due to nonlinearity of the material, this resulting in higher harmonics. Thus, the received signal consists of not only a fundamental frequency wave, but also either the second wave or higher harmonics. The nonlinear parameter associated with amplitudes of the fundamental wave and the second harmonic [21,22] is determined as follows:

$$\beta = \frac{A_2}{A_1}, \tag{8}$$

where A_1 and A_2 are amplitudes of the fundamental wave and the second harmonic wave respectively.

Thus, the nonlinearity of propagation of ultrasonic waves in rock, which is determined by the presence of cracks and pores, can be evaluated by specifying the amplitudes of the fundamental, second, and higher harmonics. To obtain a qualitative assessment of nonlinearity of this process, all the values should be normalized to represent only a relative change of the acoustic nonlinear response.

The obtained results support the conclusion that the second- and third-order nonlinearities should be evaluated to adjust the velocities of ultrasonic waves in identifying geological and mineralogical characteristics of rocks to eliminate errors associated with cracks and pores.

3. Results

Considering the above, the results of measuring the propagation of ultrasonic waves in iron ore raw materials will be assumed to be the main parameters for identifying their mineralogical and technological varieties by methods of crisp and fuzzy clustering.

Let us analyze characteristics of seven ore types that are mined and processed from one of Kryvyi Rih iron ore basin deposits. Table 4 shows the results of this analysis. The following symbols of ore types are adopted [1,12]: 1 – magnetite hornstones; 2 – silicate-carbonate-magnetite hornstones; 3 – red-striped magnetite and hematite-magnetite hornstones; 4 – semi-oxidized and oxidized hornstones; 5 – silicate shales, non-metallic hornstones and quartz; 6 – magnetite-silicate-carbonate (poor) hornstones; 7 – hematite-magnetite hornstones.

Table 4
Analysis results of different ore types

Ore type	Quartz, %	Magnetite, %	Martite, %	Hematite, %	Siderite, %	Density, kg/m^3
1	63.7	30.9	0	1.4	3.8	3431
2	68.4	21.7	0	0.4	9.1	3248
3	64.5	30.2	0	1.5	3.8	3414
4	65.4	24.4	3.3	3.7	3.2	3412
5	74.6	4.5	0	0.7	20.2	2989
6	75.2	6.8	0	0.8	17.2	3009
7	60.8	31.4	0	5.4	2.5	3530

The data used to identify mineralogical and technological varieties of iron ore by crisp and fuzzy clustering methods are observations of *the physical process of ultrasonic wave propagation in the studied medium*: Each observation consists of *n* measured variables grouped into an *n*-dimensional vector,

$$x_k = [x_{k1}, x_{k2}, \dots, x_{kn}]^T, x_k \in R^n . \tag{9}$$

The set of *N* observations is denoted by:

$$X = \{x_k | k = 1,2, \dots, N\} , \tag{10}$$

and presented as a matrix $N \times n$:

$$X = \begin{bmatrix} x_{11} & \cdots & x_{1n} \\ \vdots & \ddots & \vdots \\ x_{N1} & \cdots & x_{Nn} \end{bmatrix}. \tag{11}$$

The following rigid clustering methods have been studied: k-means and k-medoid; the fuzzy c-means (FCM) algorithm; the Gustafson-Kessel method as an advanced standard fuzzy c-means algorithm with the adaptive distance norm; the Gath-Geva method as a clustering algorithm of fuzzy maximum likelihood estimates (FMLE) which uses the distance norm based on fuzzy maximum likelihood estimates; the Fuzzy c-Shape method which replaces the norm of the internal product in the FCM model with a shape-based distance function. Figure 3 shows the results of clustering by this algorithm.

The research results indicate that the most effective method for solving this problem is the Fuzzy c-Shape method, which identifies geological and mineralogical varieties of iron ore with a 0.91% probability.

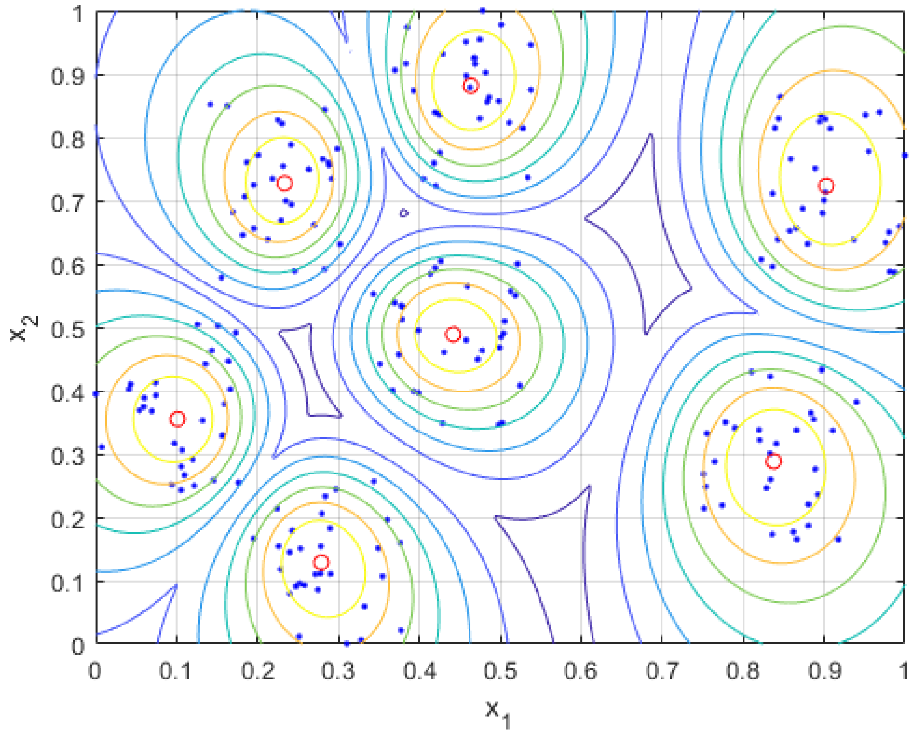

Figure 3: Clustering results using the Fuzzy c-Shape algorithm

4. Conclusion

It is established that evaluated changes in the propagation velocity of longitudinal and transverse ultrasonic bulk waves, the relationship of these values in the controlled medium and the parameter characterizing the nonlinearity degree of this process – the value of ultrasonic attenuation at fundamental and higher harmonics – can be used to identify geological and mineralogical varieties (types) of iron ore raw materials.

The proposed method based on the results of ultrasonic measurements of rock characteristics and the fuzzy inference allows identifying mineralogical and technological ore varieties in the rock massif at the initial stage of the technological process of ore extraction and processing. The specified varieties can be compared with relevant technological regulations and predetermined optimal characteristics of technological units, thus ensuring achievement of set indicators of mining and processing considering requirements of environmental protection and energy efficiency.

By comparative analysis of different crisp and fuzzy clustering algorithms, it is found that the best results in terms of accuracy and efficiency are provided by the Fuzzy c-Shape method, which replaces the norm of the internal product in the FCM model with a shape-based distance function.

5. References

1. S. Pysmenniy, N. Shvager, O. Shepel, K. Kovbyk, O. Dolgikh, Development of resource-saving technology when mining ore bodies by blocks under rock pressure, E3S Web of Conferences 166 (2020) 02006. doi: 10.1051/e3sconf/202016602006.
2. X. Pan, Optimization of mineral processing plant through ROM ore size, AGH Journal of Mining and Geoengineering 36.4 (2012) 123-132.

3. V. M. Bowa, Optimization of blasting design parameters on open pit bench a case study of nchanga open pits, International journal of scientific & technology research 4.9 (2015) 45-51.
4. Z.Q. Yue, C.F. Lee, K.T. Law, L.G. Lam, Automatic monitoring of rotary percussive drilling for ground characterization, International Journal of Rock Mechanics & Mining Sciences 41 (2015) 573–612.
5. H. Schunnesson, Rock characterisation using percussive drilling, International Journal of Rock Mechanics & Mining Sciences 35.6 (2014) 711–725.
6. H. Schunnesson, K. Holme, Drill monitoring for geological mine planning in the Viscaria copper mine Sweden, CIM Bulletin 90.1030 (2015) 82-89.
7. N. Beattie, Monitoring-while-drilling for open-pit mining in a hard rock environment: Master`s thesis. Kingston. Queen`s University. 2012. 127 p.
8. Jorge Martin. Application of Pattern Recognition Techniques to Monitoring-While-Drilling on a Rotary Electric Blast Hole Drill at an Open-Pit Coal Mine, Master's thesis, Queen`s University, Kingston, 2013.
9. J. B. Segui, M. Higgins, Blast design using measurement while drilling parameters, Fragblast: International Journal for Blasting and Fragmentation 6.3–4 (2012) 287–299.
10. M. J. Scoble, J. Peck, C. Hendricks, Correlation between rotary drill performance parameters and borehole geophysical logging, Mining Science and Technology 8 (2012) 301-312.
11. V. Morkun, N. Morkun, V. Tron, Identification of control systems for ore-processing industry aggregates based on nonparametric kernel estimators, Metallurgical and Mining Industry 7.1 (2015) 14-17.
12. V. Morkun, V. Tron, Automation of iron ore raw materials beneficiation with the operational recognition of its varieties in process streams, Metallurgical and Mining Industry 6.6 (2014) 4-7.
13. V. Morkun, N. Morkun, A. Pikilnyak, The adaptive control for intensity of ultrasonic influence on iron ore pulp, Metallurgical and Mining Industry 6.6 (2014) 8-11.
14. L. Gao, W. Zhang, W. Lu, X. Hu, H. Wu, J. Wang, B. Kong, Study on the effects of temperature and immersion on the acoustic emission and electromagnetic radiation signals of coal rock damage under load, Engineering Geology 297 (2022) 106503. doi: https://doi.org/10.1016/j.enggeo.2021.106503.
15. Acoustic properties of rocks (2017). URL: http://ctcmetar.ru/volnovye-processy/9297-akusticheskie-svoystva-gornyh-porod.html.
16. Acoustic velocity logging (2019). URL: http://fccland.ru/dobycha-nefti/6826-akusticheskiy-karotazh-po-skorosti.html.
17. X. Kou, C. Pei, Z. Chen, Fully noncontact inspection of closed surface crack with nonlinear laser ultrasonic testing method, Ultrasonics 114 (2021) 106426. doi: 10.1016/j.ultras.2021.106426.
18. H. Salehi, R. Burgueno, S. Chakrabartty, N. Lajnef, A. H. Alavi, A comprehensive review of self-powered sensors in civil infrastructure: State-of-the-art and future research trends, Engineering Structures 234 (2021) 111963. doi: https://doi.org/10.1016/j.engstruct.2021.111963.
19. F. Saati, K.-A. Hoppe, S. Marburg, K. V. Horoshenkov, The accuracy of some models to predict the acoustical properties of granular media, Applied Acoustics 185 (2022) 108358. doi: 10.1016/j.apacoust.2021.108358.
20. G. Liu, Z. Liu, J. Feng, Z. Song, Z. Liu, Experimental research on the ultrasonic attenuation mechanism of coal, Journal of Geophysics and Engineering, 14 (2017) 502–512. doi: 10.1088/1742-2140/aa5f23.
21. E.V. Trifonov, Fully integrable one-dimensional nonlinear wave equation: Solution of a general initial value problem, Partial Differential Equations in Applied Mathematics 5 (2022) 100268. doi: 10.1016/j.padiff.2022.100268.
22. M. L. Wang, J. P. Lynch, H. Sohn, Sensor Technologies for Civil Infrastructures, Woodhead Publishing, 2014.